

# Excited-State Dynamics of Carotenoids in Light-Harvesting Complexes. 1. Exploring the Relationship between the $S_1$ and $S^*$ States

Emmanouil Papagiannakis,<sup>\*,†</sup> Ivo H. M. van Stokkum,<sup>†</sup> Mikas Vengris,<sup>†,‡</sup> Richard J. Cogdell,<sup>‡</sup> Rienk van Grondelle,<sup>†</sup> and Delmar S. Larsen<sup>\*,§</sup>

Faculty of Sciences, Vrije Universiteit Amsterdam, De Boelelaan 1081, 1081 HV Amsterdam, The Netherlands, Institute of Biomedical & Life Sciences, University of Glasgow, Glasgow, United Kingdom, Department of Chemistry, University of California, Davis, One Shields Avenue, Davis, California 95616, and Faculty of Physics, Vilnius University, Sauletekio Avenue 9, Block 3, Vilnius, Lithuania

Received: August 17, 2005; In Final Form: December 7, 2005

Dispersed transient absorption spectra collected at variable excitation intensities in combination with time-resolved signals were used to explore the underlying connectivity of the electronic excited-state manifold of the carotenoid rhodopin glucoside in the light-harvesting 2 complex isolated from *Rhodospseudomonas acidophila*. We find that the  $S^*$  state, which was recently identified as an excited state in carotenoids bound in bacterial light-harvesting complexes, exhibits a different response to the increase of excitation intensity than the  $S_1$  state, which suggests that the models used so far to describe the excited states of carotenoids are incomplete. We propose two new models that can describe both the time-resolved and the intensity-dependent data; the first postulates that  $S_1$  and  $S^*$  are not populated in parallel after the decay of the initially excited  $S_2$  state but instead result from the excitation of distinct ground-state subpopulations. The second model introduces a resonantly enhanced light-induced transition during excitation, which promotes population to higher-lying excited states that favors the formation of  $S^*$  over  $S_1$ . Multiwavelength target analysis of the time-resolved and excitation-intensity dependence measurements were used to characterize the involved states and their responses. We show that both proposed models adequately fit the measured data, although it is not possible to determine which model is most apt. The physical origins and implications of both models are explored.

## 1. Introduction

Carotenoids are pigments abundant in nature that play a number of important physiological roles, including free radical scavenging,<sup>1</sup> nonphotochemical quenching,<sup>2</sup> and light-harvesting (LH) in the photosynthetic apparatuses of plants and bacteria.<sup>3</sup> Their spectroscopic properties and functions are, to a large extent, determined by their backbone of conjugated  $\pi$ -electrons.<sup>4,5</sup> The carotenoids bound in LH proteins absorb blue-green sunlight and subsequently donate the collected energy to nearby bound (bacterio)chlorophyll (BChl) molecules, from where the energy flows to the reaction center protein that mediates the ensuing charge separation reaction.<sup>6</sup> The traditionally established perspective of carotenoid electronic structure is that the excited-state manifold has two low-lying electronic states:  $S_2$  and  $S_1$  ( $1B_u^+$  and  $2A_g^-$  in polyene notation).<sup>4,5</sup> Because the  $S_1$  state has the same electronic symmetry as the ground electronic state  $S_0$  ( $1A_g^-$ ), it is a one-photon symmetry-forbidden transition and is “dark”; i.e., it is not observed in the ground-state absorption spectrum. The strong absorption of blue-green light by carotenoids corresponds to the symmetry-allowed transition from the ground state to the second excited state,  $S_2$ , and is easily observed in pump–probe (PP) measurements by a broad stimulated emission (SE) in the visible region and excited-state absorption (ESA) in the near infrared. Decay of the  $S_2$  by internal conversion (IC) populates the  $S_1$  state, which

decays to the ground state, by IC, with a lifetime that depends strongly on the conjugation length of the carotenoid (from  $\sim 1$  to  $\sim 100$  ps). The  $S_1$  state is easily observed and characterized in PP signals because of its distinct and strong ESA in the visible region.<sup>4,5</sup>

The assignment of additional temporal components and spectral evolution observed in recent PP measurements in some carotenoid-containing systems has been hotly debated. A subpicosecond component, which has been observed during the  $S_2$ – $S_1$  relaxation both in solution<sup>7,8</sup> and in LH complexes<sup>9</sup> corresponds to a blue shift of ESA in the visible within a few hundred femtoseconds and has been attributed either to vibrational relaxation within the  $S_1$  state<sup>7,8</sup> or to the population of new transient electronic states (e.g.,  $1B_u^-$ ),<sup>10</sup> whose presence was theoretically predicted earlier.<sup>11,12</sup> The observation of a component, in dispersed PP measurements, with distinct spectral and temporal signatures from  $S_1$ , led to the identification of an additional state of elusive character, the  $S^*$  state, first by Gradinaru et al.,<sup>13</sup> as a singlet excited state of spirilloxanthin in hexane and in the light-harvesting 1 (LH1) complex of *Rhodospirillum rubrum*. The next year, Papagiannakis et al.<sup>9</sup> reported the existence of  $S^*$  in spheroidene bound within the light-harvesting 2 (LH2) complex of *Rhodobacter sphaeroides*. After these initial studies, the  $S^*$  state was then observed in the LH2 complex of *Rhodospseudomonas (Rps.) acidophila*.<sup>14</sup> In these three studies, the  $S^*$  state was modeled as a direct product of  $S_2$  relaxation that is populated in parallel with the  $S_1$  state. Furthermore, the  $S^*$  state was identified as a precursor in the generation of carotenoid triplet excited states, presumably via an intramolecular singlet-fission process.<sup>11,12,15</sup> The existence

\* Authors to whom correspondence should be addressed. E-mail: papagian@nat.vu.nl; dlarsen@chem.ucdavis.edu.

<sup>†</sup> Vrije Universiteit Amsterdam.

<sup>‡</sup> University of Glasgow.

<sup>§</sup> University of California, Davis.

<sup>‡</sup> Vilnius University.

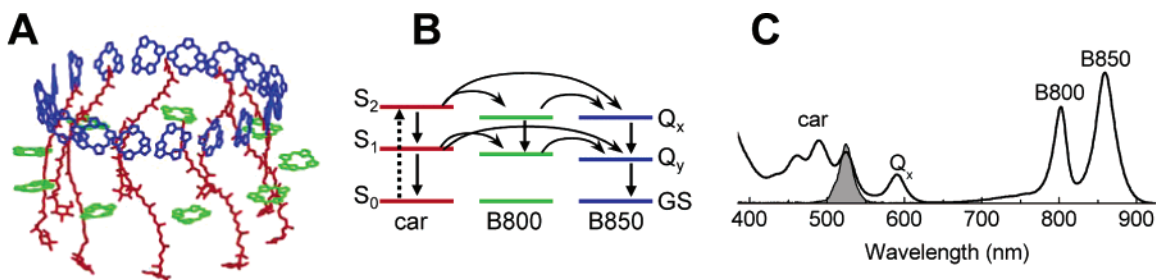


**Figure 1.** LH2 antenna complex of *Rps. acidophila*. (A) Structural arrangement of the pigments: carotenoids (red), B800 bacteriochlorophylls (green), and B850 bacteriochlorophylls (blue). (B) Highly simplified energy flow pathways from the excited carotenoid molecules to the B850 molecules, including both direct transfer and indirect transfer via the B800 bacteriochlorophylls. The thick dashed arrow represents the initial excitation of the carotenoid to the S<sub>2</sub> state. (C) Absorption spectrum of the LH2 antenna of *Rb. acidophila*. The absorption of the S<sub>2</sub> state of rhodopin glucoside is resolved around 440–550 nm (optical density at 525 nm = 0.2), and the absorption of the bacteriochlorophylls appears at 590 (Q<sub>x</sub>), 800, and 850 nm (Q<sub>y</sub>). The filled curve at 525 nm shows the spectrum of the pump laser.

of S\* contributes to a greater efficiency of excitation energy transfer (EET) from carotenoids to BChls in the *Rb. sphaeroides* LH2 complex.<sup>9</sup> The fact that the S\* state can transfer energy to the singlet excited states of BChl, together with the observation that on spirilloxanthin in solution the S\* state decays to the ground state in 5 ps and no long-lived triplets are observed,<sup>13</sup> supports the notion that the S\* is a true singlet excited state. The distinct temporal and spectral characteristics of S\* and S<sub>1</sub> suggest that they are separate electronic excited states. Even though no electronic characterization of S\* has been made so far, it was shown that its production yield and its efficiency in producing triplets is affected by the protein-imposed twist of the carotenoid backbone in the LH complex.<sup>16</sup>

To complicate matters further, other “new” excited electronic states have recently been detected in other carotenoids. In β-carotene dissolved in hexane, a new state (termed S<sup>†</sup>), which is reminiscent of S\*, was observed and characterized with dispersed multipulse transient absorption measurements;<sup>17</sup> however, the relationship between S<sup>†</sup> and S\* has not been established yet. Carbonyl-containing carotenoids have the peculiar property of generating an intramolecular charge transfer (ICT) state,<sup>18</sup> which is mostly evident in the complex carotenoid peridinin<sup>18,19</sup> bound in the peridinin–chlorophyll protein (PCP) of dinoflagellates and was recently shown to be in an excited-state equilibrium with the S<sub>1</sub> state in solution.<sup>20</sup> The electronic character and the spectroscopic properties of these “new” carotenoid excited states have yet to be fully characterized and integrated into a comprehensive model linking structure with function. Clearly, identifying the underlying connectivity of temporally overlapping states is of prime importance for interpreting their origin and understanding how and why nature selected and shaped these molecules into biological pigments.

This paper is the first in a series exploring the nature of excited-state dynamics of carotenoids in bacterial LH complexes. Here, we show how excitation-intensity-dependent dispersed PP measurements can be used to explore the relationship between the S<sub>1</sub> and the S\* states in the LH2 complex of *Rps. acidophila*. This antenna complex, whose crystal structure was resolved to atomic resolution in 1995,<sup>21</sup> features three distinct types of intrinsically bound pigments (Figure 1A): the 11-double-bond carotenoid rhodopin glucoside (red), B800 bacteriochlorophylls (green), and B850 bacteriochlorophylls (blue). Each pigment molecule exhibits multiple low-lying electronic states, which results in a complex EET network (Figure 1B).<sup>22</sup> We show that new models must be constructed to describe and interpret the measured dispersed PP data. In the second paper of the series (hereby referred to as paper 2), one such multistate model will be used to shed light on earlier optimal control results in LH2.<sup>23</sup>

## 2. Experimental Section

**2.1. Sample Preparation.** The *Rps. acidophila* 10050 LH2 complexes, isolated as described previously,<sup>24</sup> were suspended in a 20 mM Tris buffer (7.9 pH) containing 0.1% LDAO detergent. The sample had an optical density of 0.25 mm<sup>-1</sup> at 525 nm (Figure 1C) and was kept in a 1-mm quartz cuvette during the experiment, which was rapidly translated to avoid exposure to multiple laser shots. The absorption spectra of the sample measured before and after the measurements exhibited no signs of sample degradation.

**2.2 Transient Absorption Setup.** The dispersed pump–probe setup has been described in detail earlier.<sup>25,26</sup> The basis of the system is a 1-kHz amplified Ti:sapphire system delivering 450-μJ, 60-fs, 800-nm pulses. A home-built noncollinear optical parametric amplifier (NOPA) pumped by the second harmonic (400 nm) of the amplified laser system was used to generate the 40-fs, 525-nm pump pulses to excite the LH2 complexes (Figure 1C). For 800-nm excitation, the output of the amplifier was used directly. The white-light continuum, used for broadband probing, was generated by focusing a weak 800-nm beam into a slowly translating CaF<sub>2</sub> crystal. Reflective optics were used to steer and focus the probe beam into the sample, which reduced the group velocity dispersion to ~200 fs over the 450–650 nm probe region. The relative polarization of the pump and probe pulses was set to the magic angle (54.7°), and the pump and probe spot sizes at the focus were ~200 and ~50 μm, respectively. After the spatial overlap of the beams in the sample, the white-light probe pulse was dispersed with a spectrograph onto a home-built diode array detector. The collected data have a ~1-nm wavelength resolution with an average noise level of <0.5 mOD, and the instrument response function, which is limited by the probe light duration, is ~120 fs.

## 3. Results

**3.1. Time-Resolved Pump–Probe Signals.** To study the excited-state connectivity of rhodopin glucoside and BChl in the LH2 of *Rps. acidophila*, we collected spectrally resolved PP signals, which are nearly identical to previously reported data.<sup>14,27</sup> Excitation with 525-nm photons promotes rhodopin glucoside in LH2 to its S<sub>2</sub> state, which is manifested by the appearance of a strong negative ground-state bleach (GSB) below 550 nm and SE bands extending above 600 nm (Figure 2A). The decay of S<sub>2</sub> is rapid<sup>28</sup> and is correlated with the appearance of three species: the S<sub>1</sub> and S\* states (via IC) and the excited BChl (via EET). The S\* and S<sub>1</sub> populations exhibit distinct ESA bands peaking at 550 and 580 nm, respectively,

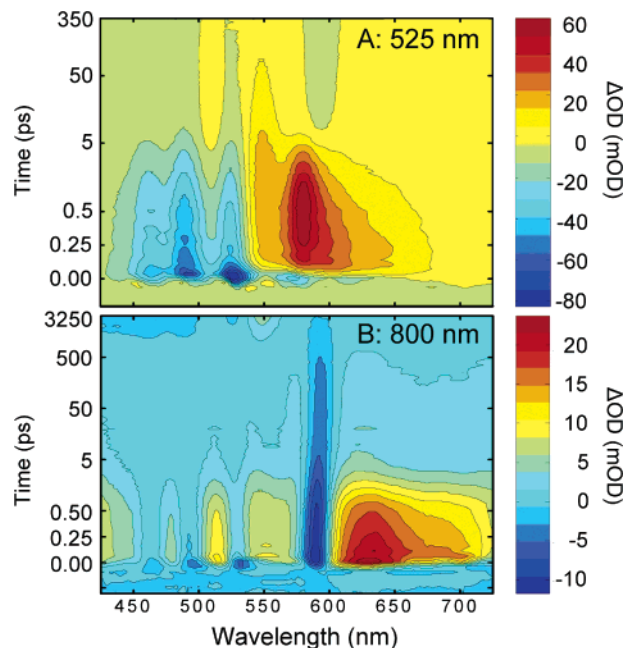


**Figure 2.** Dispersion-corrected pump-probe spectra of LH2. (A) The dynamics observed during the first 350 ps after excitation of rhodopin glucoside to the  $S_2$  state with a 525 nm pulse. The time scale (y-axis) is linear up to 0.5 ps and logarithmic from 0.5 to 350 ps. The excitation-pulse power is 60 nJ. (B) The dynamics observed after direct excitation of bacteriochlorophylls at 800 nm. The time scale is linear up to 0.5 ps and logarithmic from 0.5 ps to 3.25 ns.

and in *Rps. acidophila* this spectral separation is more appreciable than that in other  $S^*$ -exhibiting LH proteins.<sup>9,13</sup> To further complicate the relaxation dynamics, the nascent  $S_1$  state population undergoes vibrational relaxation (i.e., a blue shift of ESA) on a few hundred femtoseconds time scale before decaying by IC to the ground state with a  $\sim 3$ -ps lifetime.<sup>14,27–29</sup> In contrast, the  $S^*$  state population decays on an appreciably slower time scale into a long-lived triplet state, while the excited BChls decay on a nanosecond time scale. We will use these time-resolved data, in combination with intensity-dependent data discussed below, to model the dynamics with different models.

The proper interpretation of the PP spectra and dynamics of rhodopin glucoside in the LH2 complex requires characterizing the spectral and temporal contributions of not only the excited carotenoid signals but also the overlapping signals of excited BChls. When rhodopin glucoside is excited by 525-nm pulses, excited BChl molecules (and their signals) are produced via the rapid EET from  $S_2$  and to a smaller extent via EET from the lower energy states ( $S_1$  and  $S^*$ ) of rhodopin glucoside.<sup>14,28</sup> To characterize the contribution of the excited-state BChl in the PP signals measured in the visible region, we directly excited the B800 bacteriochlorophylls with 800-nm pulses. The resulting PP data set (Figure 2B) is distinctly different from the 525-nm excited data set and exhibits several features: (1) the  $Q_x$  bleach at 590 nm (Figure 1C), (2) a broad ESA peaking at 640 nm, (3) an electrochromic (Stark) shift of the carotenoid absorption bands around 525 nm,<sup>30,31</sup> and (4) the slowly rising carotenoid triplets at nanosecond delays, generated by the quenching of the BChl triplets formed from intersystem crossing.<sup>32</sup> These signals include dynamics of different origins, such as ultrafast  $Q_x$ – $Q_y$  relaxation,<sup>22</sup> B800–B850 energy transfer,<sup>22</sup> singlet–singlet annihilation components that appear when multiple excited BChl molecules coexist on the same LH2 ring,<sup>33,34</sup> and carotenoid triplet formation.<sup>32</sup>

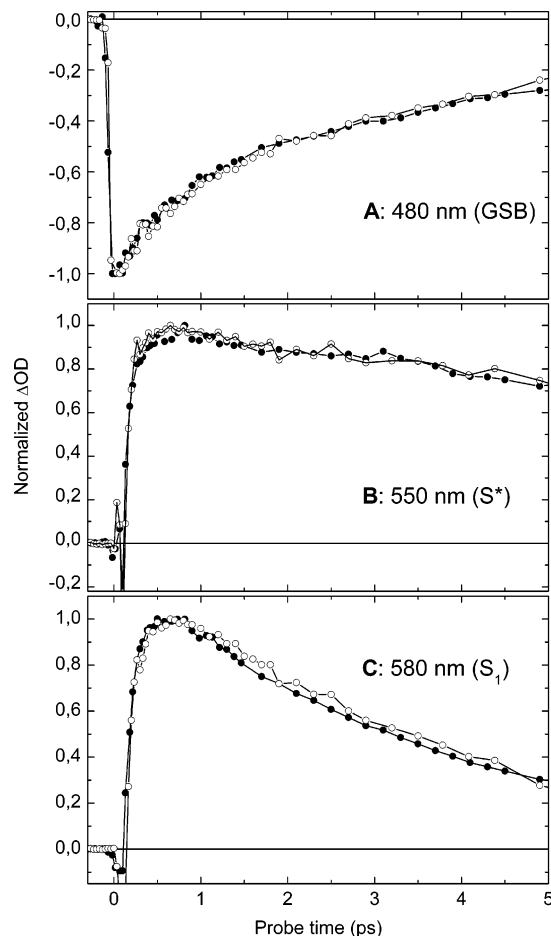


**Figure 3.** Normalized kinetic traces measured at different pulse intensities: 200 nJ/pulse (filled circles), 60 nJ/pulse (open circles). (A) Ground-state bleach probed at 480 nm, (B) the  $S^*$  ESA band probed at 550 nm, and (C) the  $S_1$  ESA at 580 nm.

**3.2. Excitation-Intensity-Dependence Measurements.** Figure 3 contrasts the dynamics measured at three characteristic wavelengths in the visible region after 525-nm excitation with low (60 nJ per pulse) and high (200 nJ per pulse) intensities. These probe wavelengths are selected because they are predominantly sensitive to the rhodopin glucoside signals with only weak contributions from overlapping BChl signals (Figure 2). At 480 nm (Figure 3A) the signal is sensitive to the carotenoid GSB and describes the magnitude of the excited-state population. At 550 and 580 nm (Figures 3B and 3C) we directly probe the population kinetics of the  $S^*$  and  $S_1$  states, and contrasting these two traces shows that the  $S^*$  population decays distinctly slower than the  $S_1$  population. At early times, a negative signal is observed in the 550- and 580-nm probe wavelength signals, which corresponds to the SE from the short-lived  $S_2$  state.<sup>28</sup> The kinetics of the populations probed at these visible wavelengths do not appear to depend on the excitation intensity.

We collected the 4-ps PP spectrum using 525-nm pulses of different intensities (Figure 4). At this probe delay, the excited-state population of rhodopin glucoside occupies either the  $S_1$  or the  $S^*$  state,<sup>14,27</sup> with a magnitude that can be directly estimated from the amplitudes of the corresponding absorption bands. The 4-ps PP spectrum exhibits four distinct spectral features in the visible region (Figure 4A): (1) the negative signal from 420 to 525 nm corresponding to the bleach of the  $S_0 \rightarrow S_2$  transition of the rhodopin glucoside molecules, (2) a positive band peaking at 550 nm that corresponds to the  $S^*$  ESA, (3) a positive band peaking at 580 nm corresponding to the  $S_1 \rightarrow S_n$

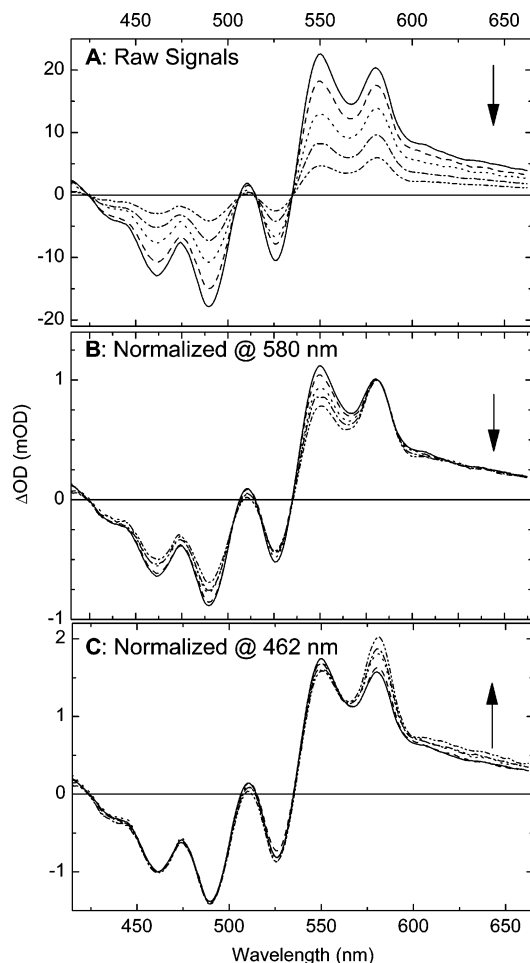


**Figure 4.** Excitation-intensity-dependent transient absorption spectra collected 4 ps after exciting rhodopin glucoside in the LH2 antenna of *Rps. acidophila* with 525-nm pulses. The pump pulse energies are 40, 85, 135, 260, and 370 nJ. (A) Raw transient absorption spectra. (B) Transient absorption spectra normalized on the peak of the  $S_1$  band at 580 nm. (C) Transient absorption spectra normalized on the peak of the ground-state bleach (GSB) band at 460 nm. The arrows indicate the trends observed with decreasing pulse intensities.

ESA transition, and (4) a weak dip at 590 nm that is ascribed to the bleach of the  $S_0 \rightarrow Q_x$  transition of the BChl molecules populated by EET from the excited carotenoids.

In contrast to the normalized decay kinetics in Figure 3, the shape of the transient absorption spectrum exhibits a pronounced intensity dependence. At low excitation intensities, the  $S_1$  ESA band at 580 nm has a greater amplitude than the  $S^*$  band at 550 nm, but as the excitation intensity increases, this relationship reverses and the amplitude of the  $S^*$  band starts to dominate the spectrum. This dependence is further illustrated when these transient spectra are normalized either on the peak of the  $S_1$  ESA band (Figure 4B) or on the blue-most peak of the GSB at 460 nm (Figure 4C). It is interesting to note that the intensity dependence of the GSB band is essentially uniform from 410 to 510 nm and the  $S_1$  ESA band responds homogeneously from  $\sim 575$  nm to 650 nm. The weak deviation observed at 590 nm can be ascribed to the effect of the decreasing relative amplitude of the  $Q_x$  bleach of BChl, originating from annihilation, which exhibits a different intensity dependence than the  $S_1$  and  $S^*$  populations (vide infra). The amplitude of annihilation, which is directly monitored at the  $Q_x$  region, is too small and at the improper wavelength to account for the pronounced intensity-dependence effect on the  $S_1$  and  $S^*$  bands in Figure 4.

Although this paper focuses on the LH2 complexes isolated from *Rps. acidophila*, similar intensity-dependent PP signals were observed in other LH complexes that exhibit  $S^*$  (Supporting Information). The normalized excitation-intensity-dependent PP spectra measured on the *Rb. sphaeroides* 2.4.1 LH2 and the *Rs. rubrum* LH1 complexes (Figure S3) reveal markedly similar properties to those of the carotenoids in these complexes (spheroidene and spirilloxanthin, respectively). This strongly supports the hypothesis that the underlying intensity dependence of the  $S^*$  and  $S_1$  bands is not unique to rhodopin glucoside in the LH2 of *Rps. acidophila* but rather a property in LH complexes in general. Furthermore, we examined the response to increasing excitation intensity of other carotenoids that exhibit “new” electronic states:  $\beta$ -carotene dissolved in hexane and peridinin dissolved in methanol (Figure S4). For  $\beta$ -carotene, we found that the response of the ESA to the increase of the intensity of the 400-nm excitation pulses was uniform across the  $S^*/S_1$  region. Similarly, in peridinin, the  $S_1$  and the intramolecular charge transfer state,<sup>18,19</sup> which is populated in polar environments, show indistinguishable intensity-dependent responses.

#### 4. Modeling and Target Analysis

In PP studies conducted with low excitation intensities, assuming a single one-photon transition, the magnitude of the excited-state populations and corresponding signals increase linearly with increasing excitation intensity. However, when more than  $\sim 10\%$  of the sample is excited,<sup>35</sup> this “linear regime” limit is exceeded and the measurement enters a “saturated regime” where the observed signals increase in a less-than-linear rate as the applied laser pulse transfers excited-state population back to the ground electronic state (e.g., via SE pumping). If there were an ESA in the Franck–Condon region of excitation, then this will lead to the “repumping” of population to higher-lying excited electronic states, the relaxation of which may open additional pathways.<sup>36</sup>

In traditional saturation measurements,<sup>35</sup> where the transient absorption signals are measured as a function of excitation intensity, all states that evolve from the same one-photon transition are expected to exhibit that same intensity dependence, and hence a uniform relative amplitude would be observed across any measured transient PP spectrum. However, the PP spectra in Figure 4, clearly show that this is not the case for LH2, and other models must be developed to properly describe the underlying photodynamics.

Three models (Figure 5) are discussed below to address the observed time-resolved and intensity-dependence signals. The corresponding set of differential equations underlying each model (Supporting Information) was solved numerically with a Runge–Kutta algorithm via the MATLAB software package and compared directly to the relevant experimental data. The homogeneous model (Figure 5A) is essentially the one used previously to describe the carotenoid dynamics in LH1<sup>13</sup> and LH2.<sup>9,14,27</sup> This model is one-photon-initiated, and the ground-state population is homogeneous. The PP data sets measured with 525- and 800-nm excitation (Figure 2) were simultaneously analyzed by target analysis (Supporting Information),<sup>37,38</sup> using this simple model, to estimate the spectrum (i.e., species-associated different spectrum, or SADS), and the time-resolved concentration profile of each constituent state of the system, including the vibrationally excited  $S_1$ ,  $S_1^*$ , and triplet states of rhodopin glucoside and the  $Q_y$  state of BChl (Figure 6).

However, models based on a single, one-photon transition, like the homogeneous model in Figure 5A, predict populations

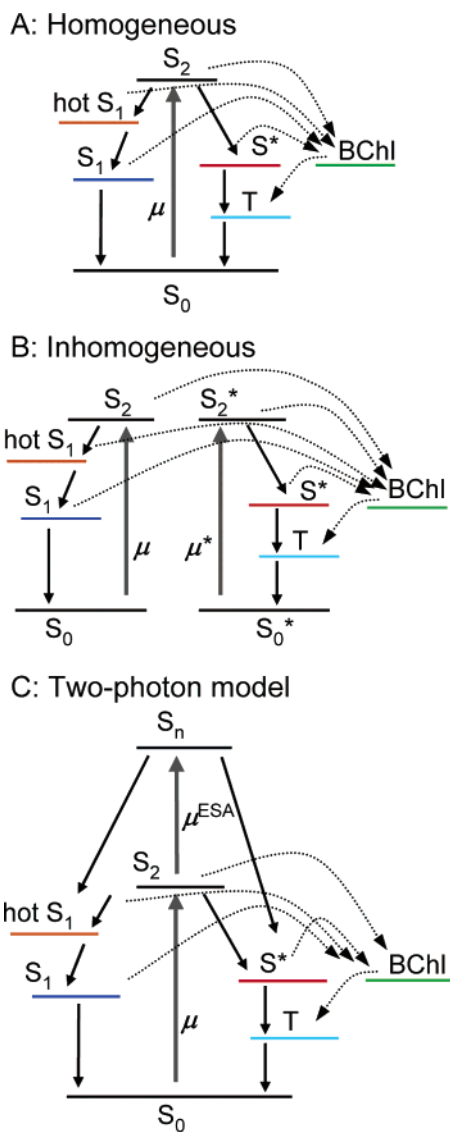


**Figure 5.** Connectivity schemes and concentrations used to interpret the light-induced dynamics in the LH2 complex. The large gray arrows represent the light-induced transitions. The small solid arrows denote the natural evolution of population, and the dotted arrows represent the singlet–singlet excitation energy transfer reactions to the bacteriochlorophyll manifold and the triplet–triplet energy transfer back to the carotenoid(s).

that exhibit *identical* intensity dependence, since they are all generated ultimately from the same transition. The saturation curves extracted from the data in Figure 4, at the peaks of  $S_1$  (blue squares),  $S^*$  (red triangles), and GSB (black circles), are shown in Figure 7A. To explain this intensity dependence we propose two new models that include multiple photon transitions occurring either sequentially (via a pump–repump process)<sup>17,20,31,39</sup> or in parallel (requiring multiple ground-state populations).

One such model is based on introducing an inhomogeneity in the ground-state population (Figure 5B). In samples that consist of multiple subpopulations with different extinction properties, the saturation measurements may be used to identify and characterize the underlying inhomogeneity (Supporting Information). Typically, the homogeneous and inhomogeneous models predict near identical population dynamics but may exhibit dissimilar intensity dependences, assuming the extinction coefficients differ appreciably for each subpopulation. In such a case, one subpopulation will saturate at a lower excitation

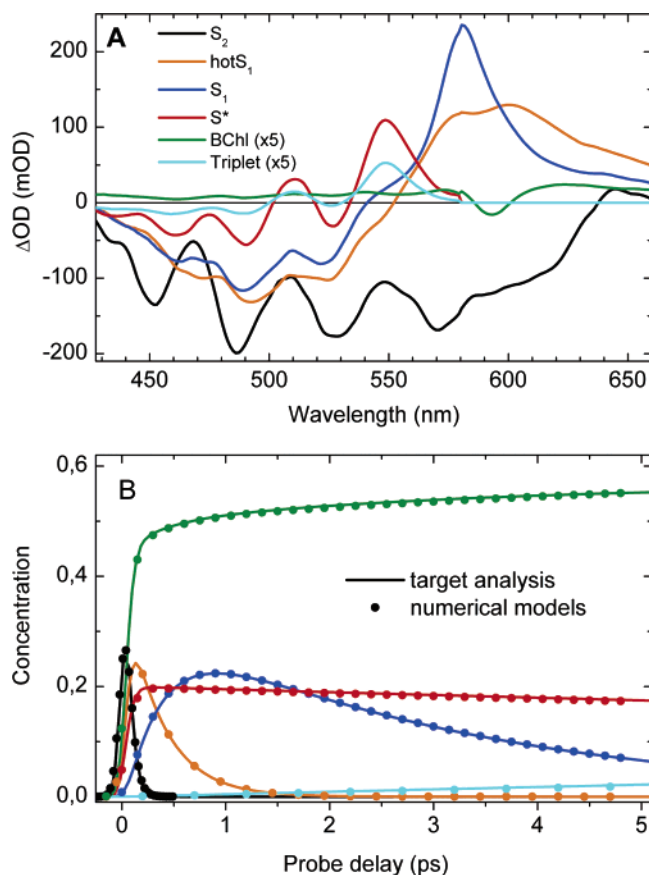


**Figure 6.** Target analysis of the time-resolved data. (A) SADS of the excited states in the LH2 antenna of *Rps. acidophila* as estimated by the combined target analysis of the 540- and 800-nm excitation data using the model in Figure 5A. (B) Time-dependent concentration profiles of the different species estimated with target analysis (solid lines) and with both the inhomogeneous and the two-photon models (symbols).

intensity than the other, thus predicting an intensity dependence similar to that in Figure 4. Within this model, the relative extinction coefficients can be characterized by simulating the different saturation behaviors of one population over the other ( $S^*$  vs  $S_1$  signals), and the relative occupation of the total ensemble can be determined by the similarity of the GSB signals to each of the other signals; i.e., the closer the saturation curve for the bleach is to a specific signal, the larger the subpopulation responsible for that signal contributes to the total population. A fit of the raw time-resolved and intensity-resolved experimental data with the inhomogeneous model in Figure 7A (dotted lines) indicates that (if this model is applicable) the ground-state population that generates  $S_1$  has a  $\sim 70\%$  greater extinction coefficient than that generating  $S^*$  and furthermore constitutes about  $\sim 40\%$  of the total ground-state population. Hence, within the context of the inhomogeneous model, more rhodopin glucoside carotenoids in LH2 of *Rps. acidophila* generate  $S^*$  than those generating  $S_1$ , albeit with a significantly smaller extinction for the ground-state absorption (Table 2).

An alternative model, which also accounts for excitation-intensity dependence, assumes a homogeneous ground state and introduces a second light-driven transition (Figure 5C). This model postulates the existence, upon excitation to  $S_2$ , of a weak ESA transition that is resonant with the 525-nm excitation pulse; consequently nascent  $S_2$  population may be “repumped” into a higher electronic state,  $S_n$ . As the excitation intensity is increased, more  $S_2$  population will be repumped into  $S_n$ , and this, combined with a branching ratio of forming the  $S^*/S_1$  states

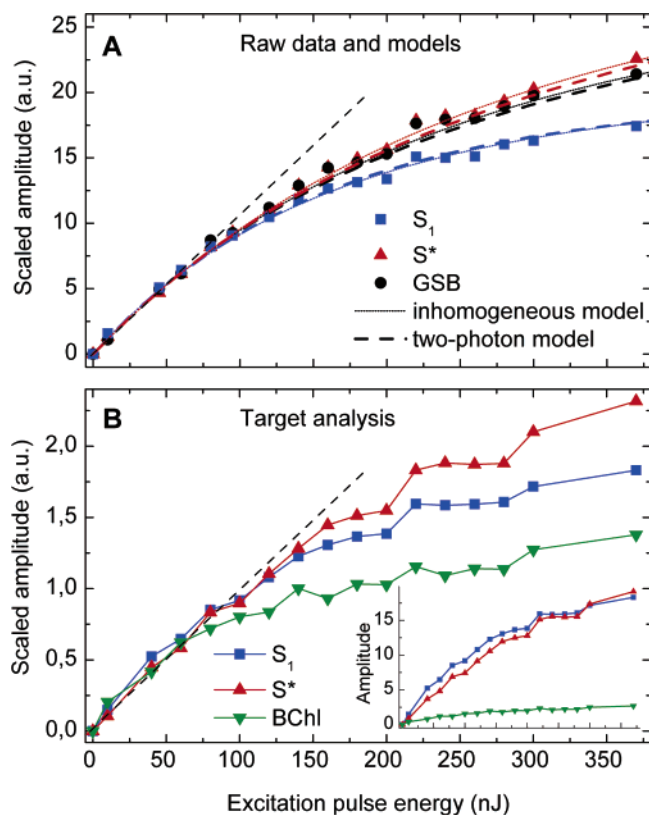


**Figure 7.** (A) Intensity-dependent amplitudes for the  $S_1$  ESA signal at 580 nm (blue squares), the  $S^*$  ESA at 550 nm (red triangles), and the bleach at 485 nm (black circles), which are scaled to the initial slope to give an initial linear dependence. The dotted lines denote the intensity dependence simulated with the inhomogeneous model of Figure 5B with a relative extinction ratio ( $S^*/S_1$ ) of 1.70 and an occupation of ( $S^*/S_1$ ) of 0.6/0.4 = 1.5. The dashed lines denote the model of the data to the two-photon model (Figure 5C) with a  $\mu_{\text{ESA}}/\mu_{\text{GSA}}$  ratio of 0.3. (B) Global analysis from time-resolved and intensity-dependent data. Excitation-intensity-dependent amplitudes of the  $S_1$ ,  $S^*$ , and BChl SADS estimated by analyzing the saturation measurement of the 4-ps PP spectrum (Figure 4). The curves have been scaled to have the same initial slope, to illustrate the different behavior of the three states; the straight dashed line is the estimated saturation-free signal. The inset contains the raw amplitudes as estimated by the fit. Note that the BChl populations (green triangles) were not resolvable from the raw data in part A and the bleach (black circles) signals were not separable from the  $S^*$  and  $S_1$  populations in the global analysis results of part B.

after the relaxation of/from  $S_n$ , which favors the formation of  $S^*$  over  $S_1$ , leads to an intensity dependence similar to that observed in the data (Figure 7A, dashes). It should be noted that since the excited-state lifetime of such  $S_n$  states have so far not been resolved,<sup>17,20,31,39</sup> the state that generates the  $S_1$  and  $S^*$  is likely a highly vibrationally excited  $S_2$  population and not the  $S_n$  state. The time-dependent populations estimated by these models for the different species present in LH2 are compared in Figure 6B. As expected, the concentration profiles predicted for all three models are essentially identical, although the underlying connectivity schemes differ appreciably (along with the corresponding kinetic parameters (Tables 1–3)). A plot highlighting the quality of the fits to the experimental data is included in the Supporting Information (Figure S2). This shows that time-resolved PP data alone is not sufficient to extract the underlying model for the 525-nm photoinduced dynamics of the rhodopin glucoside carotenoid within the LH2 complex isolated from *Rps. acidophila*.

As a test of the robustness of the target analysis of the time-resolved and intensity-dependent PP data, the SADS estimated for only the states that coexist at 4 ps,  $S_1$ ,  $S^*$ , and excited BChl, were used as a basis to fit, by multiple linear regression, the excitation-intensity-dependent 4-ps PP spectra (Figure 4) and estimate their intensity-dependent amplitudes (inset in Figure 7B). The  $S_1$  (blue squares) and  $S^*$  (red triangles) intensity-dependent amplitudes compare well with the raw data shown in Figure 7A, because the peaks of  $S_1$  and  $S^*$  are essentially free of overlapping contributions from each other. The different excitation-intensity dependences estimated from the global analysis decomposition are illustrated in Figure 7B, where the three intensity-dependent PP signals have been scaled to exhibit similar behavior in the “linear”, i.e., low excitation intensity, regime. In this analysis, the bleach signal was not separated from the excited-state signals, and thus the relative percentage of the ground-state populations cannot be directly identified (although the relative extinction coefficients can be). The BChl signal exhibits a significantly different intensity-dependent curve than both  $S_1$  and  $S^*$  signals, which is due to the additional contribution of annihilation effects<sup>34,40</sup> within the BChl manifold. The differing intensity dependences have consequences for the determination and interpretation of the photophysical properties (e.g., EET yields) of LH2; these effects will be addressed in the context of optimal control experiments in paper 2.

## 5. Discussion

Because dispersed PP signals are intrinsically self-referenced, i.e., the amplitude of a signal measured at one wavelength is directly correlated to the amplitude of the signal at another wavelength, subtle differences in the intensity dependence measurements can be identified and subsequently characterized, as in Figure 4. Such measurements on the LH2 complex of *Rps. acidophila* show that the relative amplitude of the  $S_1$  and  $S^*$  populations exhibits a clear dependence on excitation intensity. A markedly similar behavior was also observed in LH complexes from other purple bacteria (Supporting Information), indicating that this phenomenon is not unique to *Rps. acidophila* or rhodopin glucoside but rather a general aspect of carotenoids in LH proteins. The EET yields from  $S_1$  and  $S^*$  to BChl are different;<sup>9,14</sup> therefore a direct consequence of the intensity dependence of the  $S_1/S^*$  formation ratio is that the measured EET yields are unreliable at higher excitation intensities.

In this paper, we constructed two fundamentally different new models that reproduce both the experimental time-resolved and excitation-intensity-dependence properties of the PP signals. The first model entails the assumption that the ground-state population of the carotenoids in LH2 is intrinsically inhomogeneous and multiple one-photon interactions (one for each subpopulation) will lead to the observed intensity dependencies. The second, and somewhat simpler, model does not necessitate the introduction of an inhomogeneity but does require that a two-photon process occurs within the excitation pulse that modulates the  $S_1/S^*$  branching yield from either a higher-lying electronic state or the vibrationally excited  $S_2$  state. The interpretations of these models are intrinsically different, and therefore we will address the underlying features and feasibility of each model individually.

**5.1. One-Photon Model: Origins of Inhomogeneity.** The inhomogeneous model constructed in section 4 corresponds to the “extreme inhomogeneous situation” where one subpopulation of carotenoids generates *only*  $S^*$  and the other *only*  $S_1$ . Even though this model mandates the presence of a ground-state inhomogeneity, just how this inhomogeneity generates the  $S_1$

**TABLE 1: Homogeneous Model Parameters<sup>a</sup>**

	S <sub>2</sub>	hot S <sub>1</sub>	S <sub>1</sub>	S*	trip	BChl
$\tau_{\text{effective}}$	40 fs	350 fs	3 ps	30 ps	$\infty$	1.5 ns
branching yields	35% (hot S <sub>1</sub> )	3% (BChl)	20% (BChl)	80% (trip)		
	20% (S*)	97% (S <sub>1</sub> )	80% (S <sub>0</sub> )	20% (BChl)		
	45% (BChl)					

<sup>a</sup> Estimated parameters of the time-resolved dynamics obtained from the simultaneous fitting the 525- and 800-nm excitation data in Figure 2 with the homogeneous model in Figure 5A. Note that this model does not fit the intensity-dependent data in Figure 4.

**TABLE 2: Inhomogeneous Model Parameters<sup>a</sup>**

	S <sub>2</sub>	S <sub>2</sub> *	hot S <sub>1</sub>	S <sub>1</sub>	S*	trip	BChl
$\tau_{\text{effective}}$	56 fs <sup>b</sup>		350 fs	3 ps	30 ps	$\infty$	1.5 ns
$\tau$	100 fs (hot S <sub>1</sub> )	100 fs (S*)	420 fs (S <sub>1</sub> )	3.3 ps (S <sub>0</sub> )	40 ps (trip)	$\infty$	1.5 ns
	100 fs (BChl)	150 fs (BChl)	2.2 ps (BChl)	40 ps (BChl)	125 ps (BChl)		
yields	50% (hot S <sub>1</sub> )	60% (S*)	10% (BChl)	10% (BChl)	75% (trip)		
	50% (BChl)	40% (BChl)	90% (S <sub>1</sub> )	90% (S <sub>0</sub> )	25% (BChl)		

<sup>a</sup> Estimated parameters of the time-resolved dynamics obtained from simultaneously fitting the 525- and 800-nm excitation data in Figure 2 with the inhomogeneous model in Figure 5B. The ground-state population was selected from the 60 nJ excitation data. The ground-state population was set to 60% (S<sub>1</sub>)/40% (S\*), and the extinction coefficients were set to 1.7 (S<sub>1</sub>) and 1.0 (S\*), respectively. The average error for these parameters is ~10%. <sup>b</sup> Lifetime for weighted average of S<sub>2</sub> and S<sub>2</sub>\*

**TABLE 3: Two-Photon Model Parameters<sup>a</sup>**

	S <sub>2</sub>	S <sub>n</sub>	hot S <sub>1</sub>	S <sub>1</sub>	S*	trip	BChl
$\tau_{\text{effective}}$	40 fs	40 fs	350 fs	3 ps	30 ps	$\infty$	1.5 ns
$\tau$	120 fs (hot S <sub>1</sub> )	40 fs (S*)	420 fs (S <sub>1</sub> )	3.3 ps (S <sub>0</sub> )	40 ps (trip)	$\infty$	1.5 ns
	85 fs (BChl)	$\infty$ (Hot S <sub>1</sub> )	2.2 ps (BChl)	40 ps (BChl)	125 ps (BChl)		
	220 fs (S*)						
yields	33% (hot S <sub>1</sub> )	100% (S*)	10% (BChl)	10% (BChl)	75% (trip)		
	47% (BChl)	0% (Hot S <sub>1</sub> )	90% (S <sub>1</sub> )	90% (S <sub>0</sub> )	25% (BChl)		
	20% (S*)						

<sup>a</sup> Estimated parameters of the time-resolved dynamics obtained from simultaneously fitting the 525- and 800-nm excitation data in Figure 2 with the two-photon model in Figure 5C. The extinction for the S<sub>0</sub> → S<sub>2</sub> transition was set to 1.0, while for the S<sub>2</sub> → S<sub>n</sub> transition it was set at 0.3. The average error for these parameters is ~10%.

and S\* population is somewhat arbitrary, and we assume the extreme situation to maintain a relatively simple and tractable model. Different distributions can be constructed that would also describe the measured data (e.g., one with different subpopulations that branch into S\* and S<sub>1</sub> with different yields), but these would require that the ratio of the extinction coefficient be greater than the 1:1.7 ratio observed in the extreme inhomogeneous model. In the framework of this model, two distinct ground-state populations are saturating, yet the entire GSB spectrum behaves homogeneously, indicating that the underlying inhomogeneity affects only the amplitude (extinction) of the ground-state absorption spectrum and not its shape as is common in the case of disordered systems. Hence, each subpopulation must exhibit a similar, or nearly identical, absorption spectrum, albeit with significantly different ground-state extinction coefficients. Several questions require addressing regarding the feasibility of this inhomogeneous model: (1) What is the nature of this inhomogeneity? (2) How does this inhomogeneity account for the different ground-state absorption extinction coefficients (and no spectral changes)? (3) And how realistic are the extracted parameters from the model?

The carotenoid content of the LH complexes of purple bacteria has been the object of many biochemical and structural studies.<sup>41–43</sup> A potential origin for the underlying inhomogeneity could be that the carotenoid content of these LH complexes is mixed. However, the amount of carotenoids typically found in these complexes as impurities is rather small as determined from biochemical analysis<sup>41</sup> and does not account for large differences in optical properties such as the ones observed here. Alternatively, it could be argued that the inhomogeneity may correspond to the existence of cis/trans subpopulations; the determination of the structure of LH2 in 1995 speculated the presence of a

second carotenoid per structural unit,<sup>21</sup> and the recent redetermination of the structure presented stronger evidence for a population of cis carotenoids bound to the outer part of the LH2 ring, with a ~25% occupancy.<sup>44</sup> However, such a difference in the conformation of the carotenoids in the complex would lead to a distinct splitting of the absorption bands at low temperature absorption measurements, since cis carotenoids typically exhibit absorption blue-shifted by several nanometers.<sup>45</sup> The 0–1 absorption band of rhodopin glucoside in isolated LH2 complexes of *Rps. acidophila*<sup>46</sup> and of spheroidene in LH2 complexes of *Rb. sphaeroides*<sup>31</sup> is narrow and displays well-defined vibronic bands at 77 K, arguing against the coexistence of cis/trans carotenoids in the isolated LH2 complexes. This notion is further supported by resonance Raman spectroscopy, which provided little spectral evidence supporting the presence of cis rhodopin glucoside molecules in the LH2 complex of *Rps. acidophila*, in full agreement with detailed pigment analysis, finding a carotenoid/BChl ratio of 3:1.<sup>41,42</sup> Earlier linear dichroism (LD) measurements supported the existence of discrete pools of carotenoids in the LH2 complex of *Rb. sphaeroides* by measurements on both chromatophores and complexes.<sup>47,48</sup> However, no splitting of the 0–1 absorption transition was observed even in the 4 K absorption spectrum,<sup>49</sup> and the recent modeling of the 77 K absorption and circular dichroism (CD) of *Rps. acidophila* LH2 complexes did not require the introduction of such inhomogeneity.<sup>46</sup>

It is unclear how any of these potential inhomogeneities can result in such strongly differing extinction coefficients. It has been found that the S<sub>0</sub> → S<sub>2</sub> extinction coefficient among cis and trans isomers of spheroidene may vary by as much as 40%,<sup>49</sup> but as discussed above this is an unlikely case here. Furthermore, only carbonyl-containing carotenoids exhibit S<sub>0</sub> → S<sub>2</sub> absorption

extinction coefficients that depend appreciably on solvent conditions (e.g., polarity, polarizability).<sup>50–52</sup> Hence, influences from charged amino acids or the exposure of carotenoids from disrupted LH2 rings into the nonpolar detergent environment can be excluded. To complicate the study further, both extinction coefficients and excited-state lifetimes modulate saturation phenomena. In the simulations presented above with the inhomogeneous model, the analysis of the time-resolved PP data, the excited-state lifetimes of  $S_2$  and  $S_2^*$  were locked together with the same time constant (Table 1). Assuming equal extinction coefficients, an estimated lifetime of  $\sim 15$  fs is required for  $S_2$  to model the saturation curves in Figure 7A, which is unreasonably short. If the  $S_2$  lifetimes between each subpopulation were to differ, then an intensity dependence would be observed in the measured  $S_2$  lifetimes, which has not been previously explored to the authors' knowledge.

**5.2. Two-Photon Model: Excited-State Intricacy.** In contrast to the inhomogeneous model, the two-photon model does not require the introduction of inhomogeneity in the ground state but instead entails the introduction of an additional light-induced transition occurring within the excitation pulse. If the  $S_2$  population, which has a lifetime comparable to the duration of the excitation pulse, exhibits an ESA that overlaps the 525-nm excitation wavelength, then the  $S_2$  population can be subsequently promoted to a higher-lying excited state by the absorption of a second photon. Presumably, this repumped population will then be redistributed into the lower singlet state manifold (assuming no photochemistry occurs, e.g., ionization). If the  $S_1/S^*$  branching ratio in this redistribution differs from that observed after excitation to the lower vibrational levels of  $S_2$ , then, because of the multiphoton nature of this mechanism, the excitation-intensity dependencies of the  $S_1/S^*$  populations will differ. It is noteworthy that in this case, due to the excessive amount of thermal energy, the  $S^*$  state may undergo some vibrational relaxation like the  $S_1$  state,<sup>7,8</sup> which has not been observed before; however this would only be observed after mapping the excitation-dependence of the dynamics of rhodopin glucoside at early times and not just the 4-ps transient absorption spectrum (Figure 4).

It should be noted that only a true nonresonant two-photon transition will exhibit a quadratic power dependence and that any additional complexity and/or transitions (e.g., introducing an electronic state between the absorption of the two photons) will produce more a complex nonquadratic excitation-intensity dependence.<sup>26,53</sup> Once an underlying kinetic model is adopted, the corresponding excitation-intensity dependence can then be simulated, either numerically or analytically. The resulting power dependences for the two-photon model considered here are shown in Figure 7.

It is difficult to confirm the existence of the  $S_2$  ESA transition from PP measurements alone, because its observation is obscured by the strong negative GSB and SE signals in this spectral region and is further complicated by the short ( $< 100$  fs) lifetime of the  $S_2$  state.<sup>28</sup> However, it is clear that for many carotenoids in solution the GSB band does not follow the absorption spectrum exactly and is often zero at wavelengths where there is still a clear ground-state absorption (Supporting Information), which is clearer for spectra measured at later times than the  $S_2$  lifetime. The deviation of the GSB signal from the ground-state absorption spectrum indicates that there is an overlapping ESA signal with an excitation that is comparable with the ground-state extinction.<sup>17</sup> It is not surprising that a weak ESA would overlap with the spectrum of the 525-nm excitation pulses as required within the two-photon model. To fit the data

with the numerical simulations of this model (Table 3), the amplitude of the ESA needs only to be  $\sim 30 \pm 5\%$  of the amplitude of ground-state absorption, which is certainly possible. In principle, the structure and amplitude of the ESA of  $S_2$  can be examined by probing the intensity dependence of the PP signals after exciting at different wavelengths. Thus, an optimal wavelength can be identified that would minimize interfering contributions to the PP signals. Unfortunately, the ESA bands of carotenoids are typically quite broad, and such a complicated experiment may not necessarily yield positive results.

The decay of the higher,  $S_n$ , states in carotenoids appears to be extremely rapid; in previous pump–probe<sup>54</sup> and pump–repump–probe<sup>17,31,39,55</sup> experiments the higher-lying electronic state that was directly populated was not observed directly; consequently little can be said about its properties. Moreover, the consequences of exciting carotenoids beyond the  $S_2$  state, either via multiple excitations or with higher-energy photons, will vary depending on the excitation energies and the involved transitions (e.g., ionization or rapid IC). The dependence of the excited-state relaxation dynamics of carotenoids on the excitation wavelength has only been studied in solution, where the excitation of additional molecules (i.e., BChls) is avoided. Peridinin exhibits a pronounced dependence of its relaxation properties on the excitation wavelength when dissolved in protic solvents<sup>19,20</sup> but should not be considered typical because of its uniquely complex structure. Previously, it was shown that the excitation of  $\beta$ -carotene on the blue edge of its  $S_2$  absorption led to the population of an excited state,  $S^+$ , in parallel with  $S_1$ .<sup>55</sup> Even though  $S^+$  has properties not too dissimilar from the  $S^*$  state, their possible relationship was not established. Recent PP measurements on zeaxanthin<sup>54</sup> using excitation at different wavelengths showed that high-energy excitation produces transient spectra indicative of enhanced  $S^*$  population. Both studies have suggested that high-energy excitation involves overcoming a barrier along a conformational coordinate that preferentially favors the population of the  $S^+/S^*$  states. This mechanism that might also be responsible for our observations and is not ruled out by the modeling (e.g., overcoming an energetic barrier for twisting of the molecule while relaxing from the higher states). Within the framework of the two-photon model, we do not distinguish whether the branching that favors  $S^*$  occurs on the  $S_n$  state or at higher vibrational levels of the  $S_2$  state, which are populated after the relaxation of the  $S_n$  state. Although the former scenario was explicitly incorporated into the model for fitting to the measured data (since the  $S_n$  state is never really observed), these two possibilities are effectively identical.

Adopting this two-photon model has implications for the interpretation of signals from other ultrafast studies on carotenoids, either in proteins or isolated in solution. The existence of a resonantly enhanced multiphoton process (which occurs when an ESA overlaps with the excitation pulse, both temporally and spectrally) implies that in ultrafast spectroscopies the repumping of a portion of the  $S_2$  population will contribute to the signals. This is unique to ultrafast measurements where the peak excitation intensities are high, and may result in the observation of different intensity-dependent properties (e.g., spectral aspects, kinetics, or population branching yields). This ability to double pump carotenoids in ultrafast experiments allows for the possibility to induce ionization reactions.<sup>26,39,53</sup> In cases that the total excitation energy is not sufficient for ionization, other phenomena may be observed. For example, in the Cerullo et al. study of the ultrafast relaxation of  $\beta$ -carotene

in solution,<sup>56</sup> a new state, “S<sub>x</sub>”, was observed, which was interpreted as an intermediate state between S<sub>2</sub> and S<sub>1</sub>. Within the two-photon model this may be reinterpreted; the S<sub>x</sub> state can be ascribed to an S<sub>2</sub> population that is repumped by the intense and ultra-broad excitation pulse; as it is trickling down the excited-state manifold and reaches the S<sub>2</sub> state, this population may exhibit a significantly red-shifted ESA spectrum due to its highly vibrationally excited nature. This is similar to the vibrational relaxation observed in the nascent S<sub>1</sub> population following IC from S<sub>2</sub>,<sup>7,8</sup> which has significantly less excess energy (~5000 cm<sup>-1</sup>) than the repumped S<sub>2</sub> population (~20 000 cm<sup>-1</sup>).

Although both the inhomogeneous and the two-photon models adequately describe the measured intensity-dependent and time-resolved data, the feasibility of the parameters extracted from the two models requires addressing. While inhomogeneity has been observed and predicted in several LH2 complexes, the observed 70% greater extinction coefficient predicted for one subpopulation without any change in the absorption spectrum is doubtful (although not necessarily impossible). In contrast, the presence of an ESA that allows the repumping of the S<sub>2</sub> population to higher electronic state within the excitation pulse is more plausible, and a similar multipump phenomenon has been observed in dispersed PP signals from other biological systems.<sup>26,57</sup> Moreover, a 30% amplitude of the ESA relative to the GSB is sufficiently small to not be clearly observed. Although neither model can be definitively excluded, we feel the two-photon model is a more likely candidate for the appropriate LH2 model. This model is subsequently adopted in paper 2 of this series to reinterpret recent optical control experiments.

## 6. Concluding Comments

Carrying out excitation-intensity-dependent PP measurements has allowed us to gain further insight into the light-induced dynamics of the LH2 complex of *Rps. acidophila*. We have observed that the population ratio of the S<sub>1</sub> and S\* states depends on the intensity of excitation, an observation in itself important for realizing how difficult it may be to interpret simple transient absorption measurements. It is not possible to explain this observation within the previously used model to describe carotenoid dynamics from time-resolved measurements because it describes carotenoids as a uniform population or neglects the possibility for resonantly enhanced two-photon transitions that affect branching ratios. We have constructed two new models to describe the excitation-intensity dependence pump–probe experiments.

In the first model, the generation of S<sub>1</sub> and S\* populations within the rhodopin glucoside carotenoid in the LH2 of *Rps. acidophila* (and other bacterial light-harvesting complexes) is dictated by a ground-state inhomogeneity. Although the nature of such inhomogeneity is uncertain, it appears to be dynamic, not static (spectral), and hence may not necessarily be observed in many “traditional” inhomogeneity-sensitive experiments (e.g., excitation wavelength dependence studies), which are difficult to perform in the presence of other pigments, as in the LH complexes. The second model differs from the original one in that it includes a resonantly enhanced transfer of population, by the excitation pulse, from the S<sub>2</sub> state to a higher state, leading to a redistribution of the excited-state population that favors S\* formation.

Even though we cannot decide for one of the two proposed models from the PP data presented here, we postulate that in both cases the conformation of the carotenoid plays a significant

role. In the case of ground-state inhomogeneity, as was already shown, small deviations from planar configuration affect the S\* yield.<sup>16</sup> In the case of two-photon excitation, it seems quite likely that the excess excitation energy allows the molecule to access different minima along a conformational coordinate, which lead to different relaxation pathways. Consequently, attempts to understand the nature and generation of S\*, or other carotenoid “dark” states, should address the role of conformation as well as protein–carotenoid interactions.

It should be noted that although the intensity-dependent PP signals presented here cannot distinguish between the applicability of the inhomogeneous and two-photon models for the studied LH2 systems, one should be able to distinguish between these models with additional secondary measurements. Theoretically, the two models would exhibit different (single-beam) intensity dependences with respect to the observed excitation-pulse transmission. For the saturation model, the predicted pump intensity will lead to an *increased* transmission (after the sample) at elevated excitation intensities, while for the two-photon model, a *decrease* in pump transmission is expected since the ESA transition will absorb more photons at elevated excitation intensities. Performing such experiments requires the choreographing of the dispersed PP signals with the pump pulse transmission intensities, and such experiments are currently in preparation.

Irrespective of which model is applicable, we show that the application of either model, when modified with a proper description of annihilation dynamics (within the B850 population), can be used to interpret and dissect complex pulse sequences obtained from coherent control studies on LH2. This is the subject of the following paper in this series.

**Acknowledgment.** We thank Professors Neil Hunter (University of Sheffield) and Robert Niederman (Rutgers University) for generously providing the *Rb. sphaeroides* LH2 and the *Rs. rubrum* LH1 complexes discussed in the Supporting Information and Dr. Andrew Gall (University of Glasgow) and Tomáš Polívka (University of South Bohemia) for constructive discussions. This research was supported by The Netherlands Organization for Scientific Research via the Dutch Foundation for Earth and Life Sciences. D.S.L. is grateful to the Human Frontier Science Program Organization for providing financial support with both long-term and short-term fellowships.

**Supporting Information Available:** One-photon models and global analysis. This material is available free of charge via the Internet at <http://pubs.acs.org>.

**Note Added in Proof:** Two new observations lend support to the two-photon model. Kosumi et al. (*Phys. Rev. Lett.* **2005**, *95*, 213601) have recently postulated a three-state model for explaining the transient cross-phase modulation artifact in dispersed PP measurements for the  $\beta$ -carotene carotenoid in cyclohexane, which is qualitatively similar to the two-photon model proposed here. Furthermore, it has been observed that the putative ascribed cis carotenoid observed in X-ray crystallography is not a carotenoid but is really a detergent molecule (Dr. Miroslav Papiz, personal communication). Any observed inhomogeneity therefore cannot be ascribed to this source.

## References and Notes

- (1) Demmig-Adams, B.; Adams, W. W. *Science* **2002**, *298*, 2149.
- (2) Holt, N. E.; Zigmantas, D.; Valkunas, L.; Li, X. P.; Niyogi, K. K.; Fleming, G. R. *Science* **2005**, *307*, 433.
- (3) Frank, H. A.; Cogdell, R. J. *Photochem. Photobiol.* **1996**, *63*, 257.
- (4) Polívka, T.; Sundström, V. *Chem. Rev.* **2004**, *104*, 2021.

- (5) Hashimoto, H.; Yanagi, K.; Yoshizawa, M.; Polli, D.; Cerullo, G.; Lanzani, G.; De Silvestri, S.; Gardiner, A. T.; Cogdell, R. *J. Arch. Biochem. Biophys.* **2004**, *430*, 61.
- (6) van Grondelle, R.; Dekker, J. P.; Gillbro, T.; Sundström, V. *Biochim. Biophys. Acta* **1994**, *1187*, 1.
- (7) de Weerd, F. L.; van Stokkum, I. H. M.; van Grondelle, R. *Chem. Phys. Lett.* **2002**, *354*, 38.
- (8) Billsten, H. H.; Zigmantas, D.; Sundström, V.; Polívka, T. *Chem. Phys. Lett.* **2002**, *355*, 465.
- (9) Papagiannakis, E.; Kennis, J. T. M.; van Stokkum, I. H. M.; Cogdell, R. J.; van Grondelle, R. *Proc. Natl. Acad. Sci. U.S.A.* **2002**, *99*, 6017.
- (10) Koyama, Y.; Rondonuwu, F. S.; Fujii, R.; Watanabe, Y. *Biopolymers* **2004**, *74*, 2.
- (11) Tavan, P.; Schulten, K. *Phys. Rev. B* **1987**, *36*, 4337.
- (12) Tavan, P.; Schulten, K. *J. Chem. Phys.* **1986**, *85*, 6602.
- (13) Gradinaru, C. C.; Kennis, J. T. M.; Papagiannakis, E.; van Stokkum, I. H. M.; Cogdell, R. J.; Fleming, G. R.; Niederman, R. A.; van Grondelle, R. *Proc. Natl. Acad. Sci. U.S.A.* **2001**, *98*, 2364.
- (14) Wohlleben, W.; Buckup, T.; Herek, J. L.; Cogdell, R. J.; Motzkus, M. *Biophys. J.* **2003**, *85*, 442.
- (15) Rademaker, H.; Hoff, A. J.; Vangrondelle, R.; Duysens, L. N. M. *Biochim. Biophys. Acta* **1980**, *592*, 240.
- (16) Papagiannakis, E.; Das, S. K.; Gall, A.; van Stokkum, I. H. M.; Robert, B.; van Grondelle, R.; Frank, H. A.; Kennis, J. T. M. *J. Phys. Chem. B* **2003**, *107*, 5642.
- (17) Larsen, D. S.; Papagiannakis, E.; van Stokkum, I. H. M.; Vengris, M.; Kennis, J. T. M.; van Grondelle, R. *Chem. Phys. Lett.* **2003**, *381*, 733.
- (18) Bautista, J. A.; Hiller, R. G.; Sharples, F. P.; Gosztola, D.; Wasielewski, M.; Frank, H. A. *J. Phys. Chem. A* **1999**, *103*, 2267.
- (19) Zigmantas, D.; Hiller, R. G.; Yartsev, A.; Sundström, V.; Polívka, T. *J. Phys. Chem. B* **2003**, *107*, 5339.
- (20) Papagiannakis, E.; Larsen, D. S.; van Stokkum, I. H. M.; Vengris, M.; Hiller, R. G.; van Grondelle, R. *Biochemistry* **2004**, *43*, 15303.
- (21) McDermott, G.; Prince, S. M.; Freer, A. A.; Hawthornthwaite-Lawless, A. M.; Papiz, M. Z.; Cogdell, R. J.; Isaacs, N. W. *Nature* **1995**, *374*, 517.
- (22) Sundström, V.; Pullerits, T.; van Grondelle, R. *J. Phys. Chem. B* **1999**, *103*, 2327.
- (23) Herek, J. L.; Wohlleben, W.; Cogdell, R. J.; Zeidler, D.; Motzkus, M. *Nature* **2002**, *417*, 533.
- (24) Fraser, N. J.; Dominy, P. J.; Ucker, B.; Simonin, I.; Scheer, H.; Cogdell, R. *J. Biochemistry* **1999**, *38*, 9684.
- (25) Gradinaru, C. C.; van Stokkum, I. H. M.; Pascal, A. A.; van Grondelle, R.; van Amerongen, H. *J. Phys. Chem. B* **2000**, *104*, 9330.
- (26) Larsen, D. S.; Vengris, M.; van Stokkum, I. H. M.; van der Horst, M.; de Weerd, F. L.; Hellingwerf, K. J.; van Grondelle, R. *Biophys. J.* **2004**, *86*, 2538.
- (27) Rondonuwu, F. S.; Yokoyama, K.; Fujii, R.; Koyama, Y.; Cogdell, R. J.; Watanabe, Y. *Chem. Phys. Lett.* **2004**, *390*, 314.
- (28) Macpherson, A. N.; Arellano, J. B.; Fraser, N. J.; Cogdell, R. J.; Gillbro, T. *Biophys. J.* **2001**, *80*, 923.
- (29) Polívka, T.; Zigmantas, D.; Herek, J. L.; He, Z.; Pascher, T.; Pullerits, T.; Cogdell, R. J.; Frank, H. A.; Sundström, V. *J. Phys. Chem. B* **2002**, *106*, 11016.
- (30) Herek, J. L.; Polívka, T.; Pullerits, T.; Fowler, G. J. S.; Hunter, C. N.; Sundström, V. *Biochemistry* **1998**, *37*, 7057.
- (31) Wohlleben, W.; Buckup, T.; Hashimoto, H.; Cogdell, R. J.; Herek, J. L.; Motzkus, M. *J. Phys. Chem. B* **2004**, *108*, 3320.
- (32) Bittl, R.; Schlodder, E.; Geisenheimer, I.; Lubitz, W.; Cogdell, R. *J. Phys. Chem. B* **2001**, *105*, 5525.
- (33) van Grondelle, R. *Biochim. Biophys. Acta* **1985**, *811*, 147.
- (34) Trinkunas, G.; Herek, J. L.; Polívka, T.; Sundström, V.; Pullerits, T. *Phys. Rev. Lett.* **2001**, *86*, 4167.
- (35) Demtröder, W. *Laser Spectroscopy*, 2nd ed.; Pergamon Press: New York, 1987.
- (36) Stevens, M. A.; Silva, C.; Russell, D. M.; Friend, R. H. *Phys. Rev. B* **2001**, *63*, 165213.
- (37) Holzwarth, A. R. Data Analysis in time-resolved measurements. In *Biophysical Techniques in Photosynthesis*; Amesz, J., Hoff, A. J., Eds.; Kluwer: Dordrecht, The Netherlands, 1996.
- (38) van Stokkum, I. H. M.; Larsen, D. S.; van Grondelle, R. *Biochim. Biophys. Acta* **2004**, *1657*, 82.
- (39) Papagiannakis, E.; Vengris, M.; Larsen, D. S.; van Stokkum, I. H. M.; Hiller, R. G.; van Grondelle, R., submitted for publication.
- (40) van Amerongen, H.; Valkunas, L.; van Grondelle, R. *Photosynthetic Excitons*; World Scientific: Singapore, 2000.
- (41) Gall, A.; Henry, S.; Takaichi, S.; Robert, B.; Cogdell, R., J. *Photosynth. Res.* **2005**, *86*, 25–35.
- (42) Arellano, J. B.; Raju, B. B.; Naqvi, K. R.; Gillbro, T. *Photochem. Photobiol.* **1998**, *68*, 84.
- (43) Fraser, N. J. Modified pigments and mechanisms of energy transfer in LH2 complexes from purple bacteria. Ph.D. Thesis, University of Glasgow, 1998.
- (44) Papiz, M. Z.; Prince, S. M.; Howard, T.; Cogdell, R. J.; Isaacs, N. W. *J. Mol. Biol.* **2003**, *326*, 1523.
- (45) Koyama, Y.; Takatsuka, I.; Kanaji, M.; Tomimoto, K.; Kito, M.; Shimamura, T.; Yamashita, J.; Saiki, K.; Tsukida, K. *Photochem. Photobiol.* **1990**, *51*, 119.
- (46) Georgakopoulou, S.; van Grondelle, R.; van der Zwan, G. *Biophys. J.* **2004**, *87*, 3010.
- (47) de Grooth, B. G.; Amesz, J. *Biochim. Biophys. Acta* **1977**, *462*, 247.
- (48) Kramer, H. J. M.; van Grondelle, R.; Hunter, C. N.; Westerhuis, W. H. J.; Amesz, J. *Biochim. Biophys. Acta* **1984**, *765*, 156.
- (49) Fujii, R.; Furuichi, K.; Zhang, J. P.; Nagae, H.; Hashimoto, H.; Koyama, Y. *J. Phys. Chem. A* **2002**, *106*, 2410.
- (50) Britton, G. UV/Visible Spectroscopy. In *Carotenoids*; Britton, G., Liaaen-Jensen, S., Pfander, H., Eds.; Birkaeser: Berlin, 1995; Vol. 1B, p 13.
- (51) Frank, H. A.; Bautista, J. A.; Josue, J.; Pendon, Z.; Hiller, R. G.; Sharples, F. P.; Gosztola, D.; Wasielewski, M. R. *J. Phys. Chem. B* **2000**, *104*, 4569.
- (52) Zigmantas, D.; Hiller, R. G.; Sharples, F. P.; Frank, H. A.; Sundström, V.; Polívka, T. *Phys. Chem. Chem. Phys.* **2004**, *6*, 3009.
- (53) Larsen, D. S.; van Stokkum, I. H. M.; Vengris, M.; van der Horst, M.; de Weerd, F. L.; Hellingwerf, K.; van Grondelle, R. *Biophys. J.* **2004**, *87*, 1858.
- (54) Billsten, H. H.; J. P.; Sinha, S.; Pascher, T.; Sundström, V.; Polívka, T. *J. Phys. Chem. A* **2005**, *109*, 6852.
- (55) Larsen, D. S.; Papagiannakis, E.; van Stokkum, I. H. M.; Vengris, M.; Kennis, J. T. M.; van Grondelle, R. *Chem. Phys. Lett.* **2003**, *381*, 733.
- (56) Cerullo, G.; Polli, D.; Lanzani, G.; De Silvestri, S.; Hashimoto, H.; Cogdell, R. *J. Science* **2002**, *298*, 2395.
- (57) Vengris, M.; van Stokkum, I. H. M.; He, X.; Bell, A.; Tonge, P. J.; van Grondelle, R.; Larsen, D. S. *J. Phys. Chem. B* **2004**, *108*, 4587.